This paper is published in:
B.E. Murphy, S.A. Krasnikov, A.A. Cafolla, N.N. Sergeeva, N.A. Vinogradov, J.P. Beggan, O. Lübben, M.O. Senge, and I.V. Shvets, *Growth and ordering of Ni(II) diphenylporphyrin monolayers on Ag(111) and Ag/Si(111) studied by STM and LEED.* Journal of Physics: Condensed Matter **24** (2012) 045005.

Growth and ordering of Ni(II) diphenylporphyrin monolayers on Ag(111) and Ag/Si(111) studied by STM and LEED

B E Murphy[1], S A Krasnikov[1,2,5], A A Cafolla[2], N N Sergeeva[3], N A Vinogradov[2,4], J P Beggan[2], O Lübben[1], M O Senge[3] and I V Shvets[1]

[1] Centre for Research on Adaptive Nanostructures and Nanodevices (CRANN), School of Physics, Trinity College Dublin, Dublin 2, Ireland;
[2] School of Physical Sciences, Dublin City University, Glasnevin, Dublin 9, Ireland;
[3] School of Chemistry, SFI Tetrapyrrole Laboratory, Trinity Biomedical Sciences Institute, Trinity College Dublin, Dublin 2, Ireland;
[4] MAX-lab, Lund University, Box 118, 22100 Lund, Sweden.

E-mail: krasniks@tcd.ie

Abstract
The room temperature self-assembly and ordering of (5,15-diphenylporphyrinato)nickel(II) (NiDPP) on the Ag(111) and Ag/Si(111)-($\sqrt{3} \times \sqrt{3}$)R30º surfaces have been investigated using scanning tunnelling microscopy and low-energy electron diffraction. The self-assembled structures and lattice parameters of the NiDPP monolayer are shown to be extremely dependent on the reactivity of the substrate, and probable molecular binding sites are proposed. The NiDPP overlayer on Ag(111) grows from the substrate step edges, which results in a single-domain structure. This close-packed structure has an oblique unit cell and consists of molecular rows. The molecules in adjacent rows are rotated by approximately 17° with respect to each other. In turn, the NiDPP molecules form three equivalent domains on the Ag/Si(111)-($\sqrt{3} \times \sqrt{3}$)R30º surface, which follow the three-fold symmetry of the substrate. The molecules adopt one of three equivalent orientations on the surface, acting as nucleation sites for these domains, due to the stronger molecule-substrate interaction compared to the case of the Ag(111). The results are explained in terms of the substrate reactivity and the lattice mismatch between the substrate and the molecular overlayer.

1. Introduction

The self-assembly of atoms or molecules into one- and two-dimensional surface-supported nanostructures is one of the key topics in surface science and nanotechnology [1-6]. This bottom-up approach has been widely employed over the past decade for the controlled formation of ordered molecular structures on surfaces, which can lead to mass fabrication of usable systems and novel molecule-based devices with different functionality [6-10]. A complete understanding of the mechanisms and phenomena surrounding the interaction of adsorbed molecules with different surfaces is of paramount importance. The significance of molecular/inorganic interfaces for device performance cannot be overestimated as they determine charge injection and charge flow in such molecular devices.

[5] Author to whom any correspondence should be addressed.

Due to their interesting physicochemical properties and conformational flexibility, porphyrins are widely used for fabrication of complex supramolecular structures, which are utilized in many technological applications including light-harvesting arrays for solar energy generation, sensors, molecular optoelectronic gates, photo-inducible energy or electron transfer systems, nonlinear optics and oxidation catalysts [3, 6, 8, 11-14]. Furthermore, they are essential to various natural biological processes as the main functional groups of haemoglobin and chlorophyll. To this end, porphyrin derivatives have been used to prepare a rich variety of molecular nanostructures such as clusters, wires and extended networks on different surfaces [6, 15-26]. Such nanostructures offer a number of powerful approaches for the development of molecule-based devices [1-3]. The strength of the porphyrin-surface interaction is a vital parameter for controlled assembly of these functional molecular species into ordered nanostructures [23, 27]. The nature of the bonding between porphyrins and the surface is reflected in the geometric configuration of molecules at the interface and their molecular charge distribution, and therefore can be probed by scanning tunnelling microscopy (STM).

In the present work STM and low-energy electron diffraction (LEED) are used to study the molecular self-assembly of (5,15-diphenylporphyrinato)nickel(II) (NiDPP) on two surfaces, which have different reactivities, but are related: Ag(111) and Ag/Si(111)-($\sqrt{3} \times \sqrt{3}$)R30º. The Ag/Si(111)-($\sqrt{3} \times \sqrt{3}$)R30º surface was chosen since the porphyrin-substrate interaction is expected to be intermediate in strength between that of the clean Si surfaces and the Ag(111) (or hydrogen-passivated Si) [23, 24, 27-30]. On the former surface the molecules form covalent bonds and are unable to diffuse and self-assemble into ordered structures at room temperature [30], while on the latter the molecules diffuse freely and may form islands [23, 24, 27-29]. The results of this work yield important information on the conformational behaviour and structural properties of the NiDPP monolayers depending on the porphyrin-substrate interaction. This information is vital for understanding the properties of these organometallic compounds and their utilization in molecular electronic devices.

2. Experimental

The STM experiments were performed at room temperature, using a commercial instrument (Omicron Nanotechnology GmbH), in an ultra-high-vacuum system consisting of an analysis chamber (with a base pressure of 2×10^{-11} mbar) and a preparation chamber (5×10^{-11} mbar). An electrochemically etched polycrystalline tungsten tip was used to record STM images in constant current mode. The voltage V_{sample} corresponds to the sample bias with respect to the tip. No drift corrections have been applied to any of the STM images presented in this paper. The Si(111) substrate was p-type boron-doped with a resistivity in the range 0.1 – 1.0 Ω.cm. The Si(111)-(7 × 7) surface was prepared by *in situ* direct current heating to 1520 K after the sample was first degassed at 870 K for 12 hours. The Ag/Si(111)-($\sqrt{3} \times \sqrt{3}$)R30º surface was prepared by e-beam evaporation of silver (Goodfellow Metals, 5 N) from a molybdenum crucible onto the Si substrate, which was maintained at 770 K during the deposition. The Ag(111) crystal (Surface Preparation Laboratory) was cleaned *in situ* by repeated cycles of argon ion sputtering (U = 1 kV) and annealing at 820 K. The substrate cleanliness was verified by STM and LEED before deposition of the NiDPP.

NiDPP was synthesized according to a published procedure [31]. The molecules were evaporated in a preparation chamber isolated from the STM chamber at a rate of about 0.2 ML (monolayer) per minute from a tantalum crucible in a homemade deposition cell operated at a temperature of approximately 600 K. The total pressure during porphyrin deposition was in the 10^{-10} mbar range. Before evaporation the NiDPP powder was degassed for about 10 h to remove water vapour.

3. Results and discussion

3.1. NiDPP on the Ag(111)

When deposited onto the Ag(111) surface, the NiDPP molecules self-assemble at room temperature into large well-ordered domains. At 1 ML coverage, each porphyrin macrocycle, which includes a central Ni atom, four surrounding pyrrole rings and four C atoms in the meso positions, has a flat orientation on the surface with the macrocycle plane lying parallel to the substrate. Figures 1a and 1b show typical occupied and unoccupied state STM images taken from the NiDPP monolayer, respectively. In figure 1a the phenyl substituents are seen as bright oval protrusions, while the porphyrin macrocycle appears dark. In turn, in figure 1b the individual macrocycles appear as bright protrusions, each showing a four-fold symmetry and having dimensions on the order of 1nm. Such a difference in molecular appearance in figures 1a and 1b can be attributed to a difference in the electronic structure between the porphyrin macrocycle and the phenyl substituents and their geometry on the surface. In Ni porphyrins, the first unoccupied molecular orbitals are localised within the macrocycle and include unoccupied Ni 3d states [32-34]. At a relatively small positive sample bias, electrons tunnel mainly into macrocycle states and not to phenyl rings, making the porphyrin core brighter than its substituents (figure 1b). When tunnelling occurs from a number of molecular orbitals localised within both the macrocycle and phenyl rings, the latter appear to be brighter (figure 1a). This is due to the rotated position of the phenyl rings, which makes them topographically higher than the flat porphyrin macrocycle. This simplified view does not take into account the interaction between the molecule and the substrate; however, it is assumed that this interaction is weak for the Ag(111) surface.

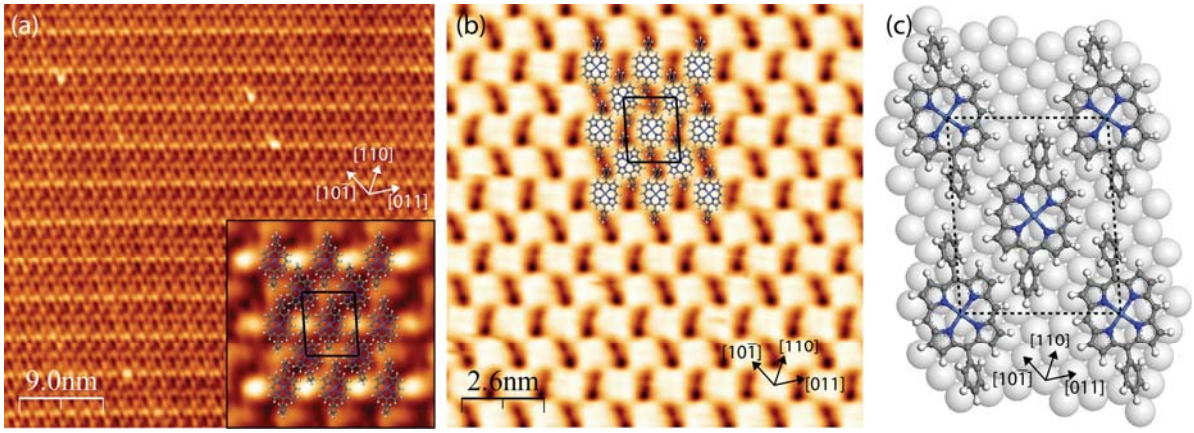

Figure 1. STM images taken from 1 ML of the NiDPP on the Ag(111) surface: (a) I_t = 0.1 nA, V_{sample} = -1.4 V, 45 nm × 45 nm and (b) I_t = 1.0 nA, V_{sample} = 1.2 V, 13 nm × 13 nm. The unit cell of the NiDPP overlayer is shown in black. Schematic representation of the NiDPP overlayer on the Ag(111) surface (c).

It is observed that each Ag(111) terrace is covered by a single molecular domain with terrace widths of up to 100 nm. The NiDPP overlayer has an oblique close-packed structure and consists of alternating molecular rows. The molecules along each row are aligned parallel to each other, while the molecules in adjacent rows are rotated by approximately 17° with respect to each other. This leads to the tilted-row pattern seen in figure 1b, arising from pairs of phenyl rings aligned with one another. The proposed model of the NiDPP monolayer on the Ag(111) surface is shown in figure 1c. The unit cell of the NiDPP lattice has the following parameters: a = 2.00 ± 0.05 nm, b = 1.60 ± 0.05 nm, γ = 85 ± 0.5°. The formation of ordered structures of this extent indicates a low diffusion barrier for the molecules on this surface at room temperature. Furthermore, a relatively weak (van der Waals) intermolecular interaction,

involving the hydrogen atoms and phenyl rings of neighbouring NiDPP molecules dominates over a weaker bonding between the molecules and the Ag(111) substrate. It is noted that the molecules desorb from the surface at a temperature of approximately 430 K, which provides further evidence for a physisorbed system weakly bonded to the substrate.

As seen in figure 2, the NiDPP molecular rows are oriented along the substrate step edges. The steps follow one of the close-packed directions of Ag(111), denoted here as [10-1], as derived from STM and LEED measured from the clean substrate. This indicates that the overlayer growth starts from the Ag(111) step edges, which imparts a direction to the resulting molecular structure. This is a clear indication that, despite a weak molecule–substrate interaction, the Ag(111) plays a crucial role in the adsorption and arrangement of the molecules. A similar type of growth has been found for other molecular layers on surfaces with a relatively low reactivity [10, 35, 36]. As shown in the overlayer model in figure 1c, the porphyrins and the substrate form an almost perfect 2:9 coincidence structure along the [10-1] direction of the Ag(111) surface, where every second molecule along this direction coincides with every ninth silver atom. This direction coincides with the long diagonal of the NiDPP overlayer unit cell.

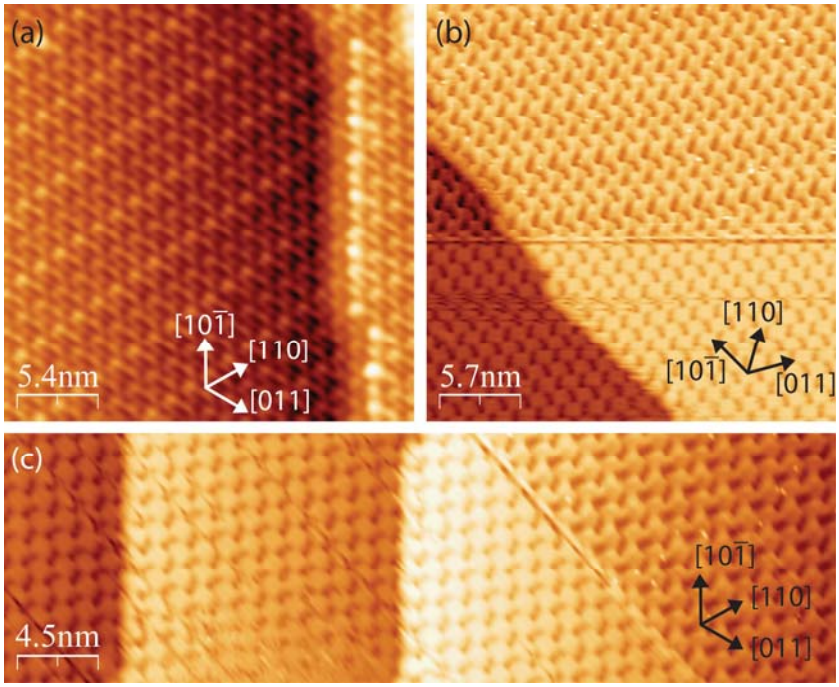

Figure 2. STM images taken from 1 ML of the NiDPP on the Ag(111) surface: (a) I_t = 0.1 nA, V_{sample} = -1.4 V, 27 nm × 27 nm, (b) I_t = 1.0 nA, V_{sample} = 1.25 V, 28 nm × 28 nm and (c) I_t = 1.0 nA, V_{sample} = 1.25 V, 50 nm × 12 nm.

All STM images of NiDPP on the Ag(111) surface show a close-packed structure of the self-assembled layer with a relatively small separation between the molecules. This is a result of significant rotation of the phenyl rings, imaged as oval protrusions (figures 1a and 1b). The plane of the phenyl rings is usually rotated by approximately 60º with respect to the macrocycle plane according to *ab initio* calculations, STM and x-ray absorption experiments [24, 30, 37, 38]. Such rotation allows the NiDPP molecules to approach each other on the surface in a specific manner and form an extended close-packed structure to minimize the surface energy.

Figure 3a shows a LEED pattern obtained from 1 ML of NiDPP deposited on the Ag(111) surface. This LEED pattern with an oblique unit cell exhibits excellent agreement

with the two-dimensional fast Fourier transform (2D-FFT) (figure 3b) of the STM images. This implies that the surface is covered by a single domain and that the STM images included are representative of the overlayer structure.

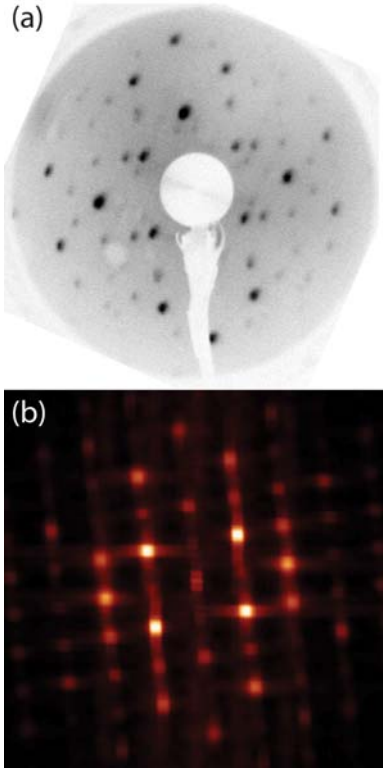

Figure 3. LEED pattern from 1 ML of the NiDPP on the Ag(111) surface, acquired at a kinetic energy of 15 eV (a). Two-dimensional fast Fourier transform calculated from the STM image shown in figure 1a (b).

3.2. NiDPP on the Ag/Si(111)-(√3 × √3)R30º

The silver-passivated Si(111) surface has a (√3 × √3)R30º reconstruction and consists of the honeycomb-chain trimer structure [39, 40]. The reactivity of this surface lies between that of the Ag(111) and the clean Si(111). It is expected that the NiDPP interaction with the Ag/Si(111)-(√3 × √3)R30º surface will be stronger than that for Ag(111), but weaker than that of the clean Si(111) surface, to allow diffusion of the molecules and the formation of ordered structures. Figure 4a shows a typical STM image of a monolayer of NiDPP molecules deposited on the Ag/Si(111)-(√3 × √3)R30º surface. The NiDPP molecules form a close-packed structure of dimer rows on this surface. There are three domains, labelled A, B and C, observed on the same terrace in figure 4a. All domains have a similar pseudo-hexagonal structure and are rotated by 120° relative to each other following the three-fold symmetry of the underlying substrate. The inset in figure 4a shows in detail the close-packed structure of one domain (A).

The existence of three different domain orientations on the same terrace of the Ag/Si(111)-(√3 × √3)R30º surface, in contrast with single-domain terraces for Ag(111), implies a much stronger molecule-surface interaction, as expected for the more-reactive Ag-passivated Si(111) surface. When deposited at room temperature, the movement of the molecules on the surface is restricted, with preferential binding sites dictated by the pseudo-hexagonal structure of the underlying surface. The NiDPP phenyl rings, which are rotated by approximately 60º with respect to the macrocycle plane, are situated closer to the Ag/Si(111)-(√3 × √3)R30º surface and most likely bonded through their hydrogen atoms to the Si trimers of the substrate. This results in an oblique (pseudo-hexagonal) unit cell with lattice parameters of 1.4 ± 0.1 nm × 1.3 ± 0.1 nm at an angle of 60 ± 2°. The proposed model of the NiDPP monolayer on the Ag/Si(111)-(√3 × √3)R30º surface is shown in figure 4b. It is noted that

twice the distance between the Si trimers is equal to 1.33 nm. In order to minimize the number of non-equivalent adsorption sites and the lattice mismatch, the NiDPP monolayer is stressed on this surface. This results in a slightly denser overlayer structure compared to the one observed on the less-reactive Ag(111) surface. The packing densities of the NiDPP overlayer on the Ag/Si(111)-($\sqrt{3} \times \sqrt{3}$)R30º and the Ag(111) surfaces, calculated from the proposed models, are equal to 0.67 and 0.63 molecules per nm^2, respectively.

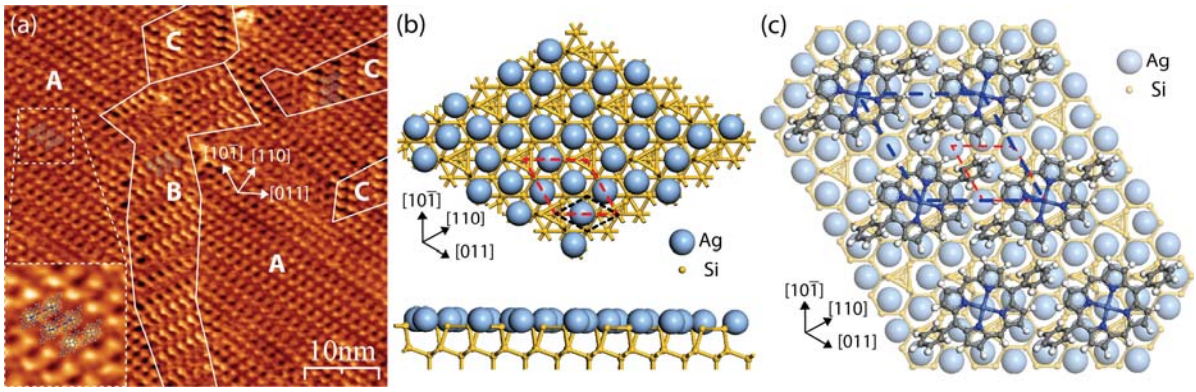

Figure 4. STM image taken from 1 ML of the NiDPP on the Ag/Si(111)-($\sqrt{3} \times \sqrt{3}$)R30º surface: I_t = 0.8 nA, V_{sample} = 1.35 V, 50 nm × 50 nm (a). Three domains of dimer rows rotated by 120° to each other are present and are labelled A, B and C in the image. The inset shows the detailed structure of one domain. Schematic representation of the Ag/Si(111)-($\sqrt{3} \times \sqrt{3}$)R30º surface (b). Schematic representation of the NiDPP overlayer on the Ag/Si(111)-($\sqrt{3} \times \sqrt{3}$)R30º surface in the case of one domain (c).

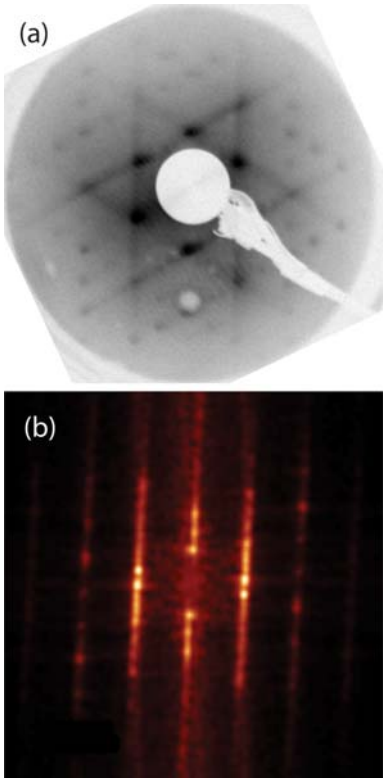

Figure 5. LEED pattern from 1 ML of the NiDPP on the Ag/Si(111)-($\sqrt{3} \times \sqrt{3}$)R30º surface acquired at a kinetic energy of 25 eV (a). Two-dimensional fast Fourier transform calculated from the STM image of one domain (A) shown in figure 4a (b).

Figure 5a shows a LEED pattern obtained from approximately 1 ML of NiDPP deposited on the Ag/Si(111)-($\sqrt{3} \times \sqrt{3}$)R30º surface. It has a pseudo-hexagonal structure confirming the presence of three domains of the molecular overlayer. By comparing the 2D-FFT calculated from the STM image of a single domain A (figure 5b) with the experimental LEED pattern, it is clear that the dominant features arise from the three equivalent domains

observed in figure 4a, oriented at 120° to one another. It is also evident from the symmetry that each orientation contributes equally to the LEED pattern, indicating that no one orientation is preferred over the others. This is in agreement with the STM data showing that the NiDPP overlayer structure consists of dimer rows growing in three equivalent directions, dictated by the hexagonal symmetry of the Ag/Si(111)-($\sqrt{3} \times \sqrt{3}$)R30º surface. The significant streaking of the LEED spots (figure 5a), which are also visible in the 2D-FFT (figure 5b), is a result of the dimer row structure observed in STM images. This streaking indicates the presence of disorder along the molecular rows and arises due to a variation in the lattice parameter of the molecular unit cell in the direction parallel to the molecular rows. This in turn is attributed to non-equivalent rotation and/or bending of the individual phenyl rings in order to minimize the lattice mismatch between the NiDPP overlayer and the substrate.

In conclusion, by using STM and LEED we have demonstrated that self-assembly of the NiDPP molecules at room temperature depends greatly on the choice of substrate. If deposited on the relatively-inert Ag(111) surface, molecule-molecule interactions dominate and the NiDPP molecules form a close-packed, single-domain monolayer, which starts to grow from the substrate step edges. In contrast, on the more-reactive Ag/Si(111)-($\sqrt{3} \times \sqrt{3}$)R30º substrate, the molecule-substrate interaction is stronger than in former case, leading the deposited molecules to adopt one of three equivalent orientations on the surface. These initial orientations act as nucleation sites for the three equivalent molecular domains distributed randomly over the substrate terraces.

Acknowledgements

This work was supported by the Irish Higher Education Authority PRTLI programme and by Science Foundation Ireland through Principal Investigator grants (Nos. 09/IN.1/I2635 and 09/IN.1/B2650). STM topographic images were processed using the WSxM software [41].

References

[1] Barth J V 2007 *Ann. Rev. Phys. Chem.* **58** 375
[2] Barth J V, Costantini G and Kern K 2005 *Nature* **437** 671
[3] Barlow S M and Raval R 2003 *Surf. Sci. Rep.* **50** 201
[4] Krasnikov S A, Hanson C J, Brougham D F and Cafolla A A 2007 *J. Phys.: Condens. Matter* **19** 446005
[5] Lübben O, Krasnikov S A, Preobrajenski A B, Murphy B E and Shvets I V 2011 *Nano Res.* **4** 971
[6] Elemans J A W, van Hameren R, Nolte R J M and Rowan A E 2006 *Adv. Mater.* **18** 1251
[7] Liang H, He Y, Ye Y C, Xu X G, Cheng F, Sun W, Shao X, Wang Y F, Li J L and Wu K 2009 *Coord. Chem. Rev.* **253** 2959
[8] Joachim C, Gimzewski J K and Aviram A 2000 *Nature* **408** 541
[9] Ikkala O and ten Brinke G 2002 *Science* **295** 2407
[10] Krasnikov S A, Bozhko S I, Radican K, Lübben O, Murphy B E, Vadapoo S-R, Wu H-C, Abid M, Semenov V N and Shvets I V 2011 *Nano Res.* **4** 194
[11] Senge M O, Fazekas M, Notaras E G A, Blau W J, Zawadzka M, Locos O B and Mhuircheartaigh E M N 2007 *Adv. Mater.* **19** 2737
[12] Lin V S Y, DiMagno S G and Therien M J 1994 *Scienc*e **264** 1105
[13] Chen J, Reed M A, Rawlett A M and Tour J M 1999 *Science* **286** 1550
[14] Tsuda A and Osuka A 2001 *Science* **293** 79
[15] Yokoyama T, Yokoyama S, Kamikado T, Okuno Y and Mashiko S 2001 *Nature* **413** 619

[16] Stepanow S, Lingenfelder M, Dmitriev A, Spillmann H, Delvigne E, Lin N, Deng X, Cai C, Barth J V and Kern K 2004 *Nature Mater.* **3** 229
[17] van Hameren R, Schon P, van Buul A M, Hoogboom J, Lazarenko S V, Gerritsen J W, Engelkamp H, Christianen P C M, Heus H A, Maan J C, Rasing T, Speller S, Rowan A E, Elemans J A W and Nolte R J M 2006 *Science* **314** 1433
[18] Spillmann H, Kiebele A, Stöhr M, Jung T A, Bonifazi D, Cheng F and Diederich F 2006 *Adv. Mater.* **18** 275
[19] Grill L, Dyer M, Lafferentz L, Persson M, Peters M V and Hecht S 2007 *Nat. Nanotechnol.* **2** 687
[20] Nishiyama F, Yokoyama T, Kamikado T, Yokoyama S, Mashiko S, Sakaguchi K and Kikuchi K 2007 *Adv. Mater.* **19** 117
[21] Bonifazi D, Kiebele A, Stöhr M, Cheng F, Jung T, Diederich F and Spillmann H 2007 *Adv. Funct. Mater.* **17** 1051
[22] Beggan J P, Krasnikov S A, Sergeeva N N, Senge M O and Cafolla A A 2008 *J. Phys.: Condens. Matter* **20** 015003
[23] Krasnikov S A, Beggan J P, Sergeeva N N, Senge M O and Cafolla A A 2009 *Nanotechnology* **20** 135301
[24] Krasnikov S A, Sergeeva N N, Sergeeva Y N, Senge M O and Cafolla A A 2010 *Phys. Chem. Chem. Phys.* **12** 6666
[25] Haq S, Hanke F, Dyer M S, Persson M, Iavicoli P, Amabilino D B and Raval R 2011 *J. Am. Chem. Soc.* **133** 12031
[26] Krasnikov S A, Doyle C M, Sergeeva N N, Preobrajenski A B, Vinogradov N A, Sergeeva Y N, Zakharov A A, Senge M O and Cafolla A A 2011 *Nano Res.* **4** 376
[27] Schnadt J, Xu W, Vang R T, Knudsen J, Li Z, Lægsgaard E and Besenbacher F 2010 *Nano Res.* **3** 459
[28] Suzuki Y, Hietschold M and Zahn D R T 2006 *Appl. Surf. Sci.* **252** 5449
[29] Auwärter W, Weber-Bargioni A, Riemann A, Schiffrin A, Gröning O, Fasel R and Barth J V 2006 *J. Chem. Phys.* **124** 194708
[30] Moriarty P J 2010 *Surf. Sci. Rep.* **65** 175
[31] Brückner C, Posakony J J, Johnson C K, Boyle R W, James B R and Dolphin D 1998 *J. Porphyrins Phthalocyanines* **2** 455
[32] Liao M-S and Scheiner S 2002 *J. Chem. Phys.* **117** 205
[33] Krasnikov S A, Preobrajenski A B, Sergeeva N N, Brzhezinskaya M M, Nesterov M A, Cafolla A A, Senge M O and Vinogradov A S 2007 *Chem. Phys.* **332** 318
[34] Krasnikov S A, Sergeeva N N, Brzhezinskaya M M, Preobrajenski A B, Sergeeva Y N, Vinogradov N A, Cafolla A A, Senge M O and Vinogradov A S 2008 *J. Phys.: Condens. Matter* **20** 235207
[35] Cuberes M T, Schlittler R R and Gimzewski J K 1998 *Appl. Phys.* A **66** S669
[36] Tang H, Cuberes M T, Joachim C and Gimzewski J K 1997 *Surf. Sci.* **386** 115
[37] Yokoyama T, Yokoyama S, Kamikado T and Mashiko S 2001 *J. Chem. Phys.* **115** 3814
[38] de Jong M P, Friedlein R, Sorensen S L, Öhrwall G, Osikowicz W, Tengsted C, Jönsson S K M, Fahlman M and Salaneck W R 2005 *Phys. Rev.* B **72** 035448
[39] Wilson R J and Chiang S 1987 *Phys. Rev. Lett.* 58 369
[40] van Loenen E J, Demuth J E, Tromp R M and Hamers R J 1987 *Phys. Rev. Lett.* **58** 373
[41] Horcas I, Fernandez R, Gomez-Rodriguez J M, Colchero J, Gomez-Herrero J and Baro A M 2007 *Rev. Sci. Instrum.* **78** 013705